Interaction of [^{125}I]-α-Bungarotoxin with Acetylcholine Receptor from *Torpedo californica*†

Steven G. Blanchard,‡ Ulrich Quast,‡,‡ Kenton Reed, Theodore Lee,§ Michael I. Schimerlik,¶ Richard Vandlen,‖ Toni Claudio, Catherine D. Strader, Hsiao-Ping Hsu Moore, and Michael A. Raftery*

ABSTRACT: The preparation and characterization of an iodinated derivative of α-bungarotoxin are described. A general method for investigation of the kinetic homogeneity of a radiolabeled toxin is presented. The kinetics of iodinated α-bungarotoxin binding to acetylcholine receptor from *Torpedo californica* are quantitatively studied in the presence and absence of cholinergic ligands by a DEAE filter disc assay (Schmidt, J., & Raftery, M. A. (1973) *Anal. Biochem. 52*, 349) which is described in detail. In the case of membrane-bound receptor, the concentration dependence of the kinetics of toxin binding was determined up to the experimentally attainable limit of 3 μM. The kinetics followed a one-step association mechanism with a single class of (non-interacting) binding sites in the membranes. The association rate constant was $(1.2 \pm 0.1) \times 10^4$ M^{-1} s^{-1}, and the lifetime of the complex was longer than 2 days. Preequilibration of the membrane-bound receptor with cholinergic ligands resulted in an apparently competitive inhibition of toxin binding. This inhibition is adequately described by simple hyperbolas without indication of heterogeneous or interacting ligand binding sites on the membrane-bound receptor. In the case of solubilized, purified receptor, the kinetics with toxin in excess were faster than those for the membrane-bound receptor and were biphasic. Perturbation of the native environment of the receptor may be the origin of the heterogeneous toxin binding kinetics.

The observation of the specific blockade of the nicotinic acetylcholine receptor in vivo by α-toxins from snake venoms (Lee & Chang, 1966; Lee et al., 1967) has greatly facilitated the characterization of these receptors at the biochemical level. Cholinergic ligands inhibit toxin binding to the solubilized, purified (Moody et al., 1973; Schmidt & Raftery, 1974; Meunier et al., 1974; Maelicke et al., 1977) and membrane-bound AcChR[1] (Weber & Changeux, 1974; Bulger et al., 1977; Quast et al., 1978b). Although the underlying molecular mechanism of this inhibition is unknown (Quast et al., 1978b), the inhibition as a function of ligand concentration is often reasonably well described by simple hyperbolas from which inhibition constants K_i can be determined (Weber & Changeux, 1974; Vandlen et al., 1976). These inhibition constants show good agreement with equilibrium constants for the interaction of ligand with AcChR as determined by other methods. Changes in ligand affinity toward membrane-bound AcChR as a functon of incubation time with ligand have been detected by the inhibition of toxin binding. These changes have been described in a qualitative (Weber et al., 1975; Lee et al., 1977) and quantitative manner (Colquhoun & Rang, 1976; Weiland et al., 1977; Quast et al., 1978b).

Although important information on the AcChR and its interaction with cholinergic ligands has been obtained by the study of the association of α-neurotoxins with the receptor, the mechanism of this interaction is still very much in question, especially in the case of membrane-bound AcChR [compare, e.g., Weber & Changeux (1974) and Quast et al. (1978b) with Bulger et al. (1977)]. In these studies, conflicting data and interpretations have been presented concerning the mechanism of toxin binding and of its inhibition by cholinergic ligands. Studying the concentration dependence of toxin binding to the membrane-bound AcChR from *Electrophorus*, Bulger et al. (1977) observed a complex kinetic pattern and concluded that toxin acted as an allosteric effector of the receptor. This is in contrast to our observation of a simple bimolecular association of toxin with AcChR from *Torpedo californica* (Quast et al., 1978b). In view of these discrepancies, it is important to carefully characterize the preparations of radiolabeled toxin and of AcChR used in the experiments and to examine the details of the assay procedure quantitatively.

In the present communication we describe the chemical characterization of our preparation of native α-BuTx and its ^{125}I derivative. The binding mechanism of the radiolabeled toxin to membrane-bound as well as solubilized AcChR from *T. californica* has been investigated, and the inhibition of toxin binding to membrane-bound AcChR equilibrated with cholinergic ligands has been examined in detail.

Experimental Section

Materials

T. californica was obtained locally. Electric organs were excised and either used immediately or frozen at −90 °C. The lyophilized venom of *Bungarus multicinctus* was obtained from Sigma Chemical Co. Whatman DEAE-cellulose filter discs (DE-81) were obtained through VWR Scientific Co. Carbamylcholine chloride, nicotine alkaloid, and *d*-tubocurarine chloride were obtained from Sigma Chemical Co., deca-

† From the Church Laboratory of Chemical Biology, Division of Chemistry and Chemical Engineering, California Institute of Technology, Pasadena, California 91125. *Received July 11, 1978; revised manuscript received December 15, 1978.* Contribution No. 5823. Supported by U.S. Public Health Service Grants NS-10294 and GM-16424, by a National Institutes of Health Predoctoral Fellowship (to S.G.B. and C.D.S), by a Deutsche Forschungsgemeinschaft Postdoctoral Fellowship (to U.Q.), and by a National Institutes of Health Postdoctoral Fellowship (to M.S. and R.V.)

‡ First two authors listed in alphabetical order.

‡ Present address: Biozentrum CH-4056, Basel, Switzerland.

§ Present address: Molecular Biology Institute, University of California, Los Angeles, Los Angeles, CA.

¶ Present address: Department of Biochemistry and Biophysics, Oregon State University, Corvallis, OR.

‖ Present address: Merck Sharp & Dohme Research Labs, Rahway, NJ 07065.

[1] Abbreviations used: AcCh, acetylcholine; AcChR, acetylcholine receptor; α-BuTx, α-bungarotoxin; [^{125}I]-α-BuTx, α-bungarotoxin iodinated with ^{125}I; DEAE, diethylaminoethyl; Carb, carbamylcholine; Deca, decamethonium; Hexa, hexamethonium; *d*-Tc, *d*-tubocurarine; DFP, diisopropyl fluorophosphate; DAP, 1,10-bis(3-aminopyridino)decane diiodide; *Torpedo* Ringer's solution, 250 mM NaCl, 5 mM KCl, 4 mM $CaCl_2$, 2 mM $MgCl_2$, and 5 mM Tris, pH 7.4; Eth, ethidium bromide; Nle, norleucine; DTT, dithiothreitol.

0006-2960/79/0418-1875$01.00/0

methonium bromide and flaxedil were from K & K Laboratories, hexamethonium chloride was from Schwarz/Mann, and ^{125}I (as NaI) was from New England Nuclear. DAP was synthesized by a modification of the method of Mooser et al. (1972).

Methods

(*1*) *AcChR.* Membrane fragments enriched in *T. californica* AcChR were prepared by zonal centrifugation as described by Duguid & Raftery (1973) and Reed et al. (1975). Solubilized receptor was prepared according to Vandlen et al. (1976).

(*2*) *Preparation and Standardization of α-BuTx.* α-BuTx was purified from the lyophilized venom by the procedure of Clark et al. (1972) with a shallower gradient (600 mL of 0.1 M NH_4Ac and 600 mL of 0.25 M NH_4Ac). The α-BuTx which constitutes the major peak of the elution profile (followed by absorption at 280 nm) was eluted at a concentration of 0.14 M NH_4Ac. The preparation was pure as judged by rechromatography. The purified toxin migrated as a single component on a heavily loaded slab gel when we used the discontinuous $NaDodSO_4$ gel system described by Laemmli (1970) with an 8–18% exponential gradient.

The activity of the toxin preparation (defined by its ability to bind to AcChR) was determined by the elution profiles of (a) toxin, (b) solubilized AcChR, and (c) a preequilibrated mixture of toxin and AcChR, with the latter in excess, on a small (4 mL) Whatman DE-52 column equilibrated with washing buffer. Protein was assayed by the Fluram method (Pierce Chemical Co.). The positively charged toxin appeared in the void volume of the column, whereas the negatively charged AcChR and the receptor–toxin complex were retarded. If the toxin preparation was completely active, no protein was expected in the void volume when the equilibrated mixture of toxin and receptor was chromatographed. From the limited resolution of the method, the toxin was judged to be more than 90% active. The molar absorptivity of the pure toxin at 279 nm was determined from a solution of carefully dried material whose toxin content was determined by amino acid analysis with Nle as an internal standard. The absorption coefficient = $(1.05 \pm 0.1) \times 10^4$ M^{-1} cm^{-1}, in good agreement with published values (Chicheportiche et al., 1975; Bulger et al., 1977). A solution of this purified toxin was prepared to serve as standard for the calibration of the radiolabeled toxin. Aliquots of this solution were sealed under vacuum in individual glass ampules and stored at −90 °C until use. The concentration of the stated standards, as determined by absorption and amino acid analysis, was 80 ± 8 μg/mL.

(*3*) *Preparation and Chemical Characterization of [^{125}I]-α-BuTx.* The purified toxin was labeled with ^{125}I by a modification of the procedure of Vogel et al. (1972). Eight milligrams of purified α-BuTx was dissolved in 2 mL of borate buffer (0.2 M H_3BO_3, 0.16 N NaOH, and 0.16 M NaCl, pH 8.0) at 0 °C. The iodinating mixture contained 10 mCi of carrier-free $Na^{125}I$ in 0.1 mL of 0.1 M NaOH, 50 μL of 0.01 M KI, 0.2 mL of 2.5 N HCl, and 40 μL of 1 M $NaNO_2$. After 5 min at 0 °C, the iodinating mixture was neutralized with 0.2 mL of 2.5 N NaOH, and the α-BuTx solution was added immediately. The iodination reaction was allowed to proceed for 4 min at 0 °C before the reaction was quenched by addition of 25 μL of 0.1 M NaS_2O_3 and 25 μL of 0.1 M NaI. The solution was immediately chromatographed on a Sephadex G-25 column (40 × 2.5 cm) equilibrated in 3.3 mM sodium phosphate buffer, pH 7.4. The elution profile was followed by counting aliquots for radioactivity and by Fluram assay for protein. All detectable protein was eluted in a void volume peak containing most of the radioactivity with a smaller protein-free radioactive peak (probably unreacted $^{125}I^-$) appearing later. The void volume peak was pooled, applied to a Sephadex CM-25 column (15 × 2 cm; equilibrated with the same buffer), and eluted with a linear gradient (200 mL of 0.02 M NaCl and 200 mL of 0.1 M NaCl in 3.3 mM sodium phosphate buffer, pH 7.4), followed by 200 mL of buffer containing 0.5 M NaCl. The elution profile is shown in Figure 1. The main peak of radioactivity containing the monoiodo- and unlabeled α-BuTx (see below) was pooled, concentrated, and desalted on a Sephadex G-25 (40 × 2.5 cm) column equilibrated in 0.1 M acetic acid, followed by lyophilization. The product was dissolved in 2 mL of 5 mM sodium phosphate buffer at pH 7.4 and passed through a Pasteur pipet column of DEAE-cellulose in order to remove any impurity which might bind to the DEAE discs used in the filter assay of Schmidt & Raftery (1973). The stock solution (≃1 mg/mL in protein) was stored frozen at −20 °C.

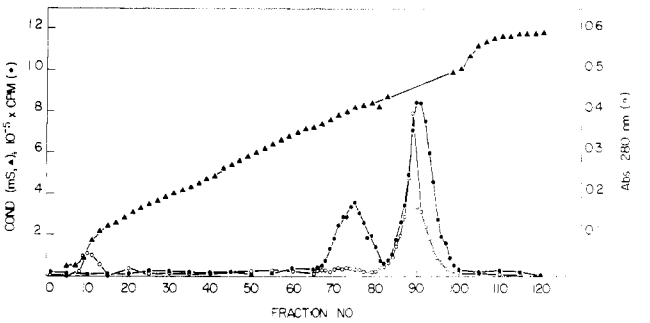

FIGURE 1: Purification of [^{125}I]-α-BuTx by chromatography on Sephadex CM-25. After desalting, monoiodo- and unlabeled α-BuTx were separated from other product(s) of the iodination reaction on Sephadex CM-25 (see Methods for details). Radioactivity (●) was determined by counting 5-μL samples in a Beckman 4000 γ counter. The radioactive peak centered at fraction 75 contained no protein as measured by absorbance at 280 nm (○) and was discarded. The peak around fraction 90 containing the monoiodo- and unlabeled toxins was collected and treated as described under Methods. The gradient was followed by measurement of the conductivity (▲).

The position of the label(s) in [^{125}I]-α-BuTx was investigated by reduction and aminoethylation of the disulfide bonds, followed by cyanogen bromide cleavage. Two radioactive preparations were examined. A trace of the radiolabeled toxin and 6 mg of unlabeled toxin were dissolved in 3 mL of 0.1 M Tris-HCl and 0.1 M sodium borate buffer at pH 8.6, containing 6 M guanidinium chloride. DTT (300 mg) was added and allowed to react for 3 h. The sulfhydryl groups were then aminoethylated by the method of Raftery & Cole (1963), and the mixture was desalted on a Sephadex G-25 column. Following lyophilization, the toxin was cleaved with cyanogen bromide (Steers et al., 1965) and relyophilized. The cyanogen bromide fragments were separated on a Sephadex CM-25 column (1.6 × 90 cm) following a modified procedure of Mebs et al. (1971, 1972). The elution profile was assayed for protein by Fluram assay and for radioactivity. In both cases, the Fluram assay showed two major peaks which were identified with the two cyanogen bromide fragments obtained by Mebs et al. (1971) in their sequencing study of α-BuTx. Radioactivity was mainly associated with the second fragment. Since a complete separation of the fragments was not achieved, it cannot be ruled out that the first fragment contained some radioactivity. The specific activity of fragment I was estimated to be less than 10 ± 10% that of fragment II. Two different preparations of radiolabeled toxin were also examined with the $NaDodSO_4$ gel system described above. Both migrated as a single band as seen by autoradiography and comigrated

with the purified unlabeled toxin. The preparation was found to be 100% active by comparison of the elution profiles on Sephadex G-25 of (a) [^{125}I]-α-BuTx and (b) a mixture of toxin with solubilized receptor (the latter in excess), since all radioactivity appeared as receptor–toxin complex. The determination of the specific activity and the concentration of the [^{125}I]-α-BuTx will be described under Results and Discussion.

(*4*) *DEAE Disc Assay.* The DEAE disc assay of Schmidt & Raftery (1973) was used to determine the concentration of (solubilized or membrane-bound) AcChR and to follow the kinetics of toxin binding. For the determination of toxin sites, 100 μL of solutions containing [^{125}I]-α-BuTx (concentration $\simeq 1 \times 10^{-7}$ M) and varying amounts of receptor were applied to DE-81 DEAE discs after a 10–30-min incubation period at room temperature. The discs were then washed with three changes, over 30 min, of washing buffer (10 mM sodium phosphate, pH 7.5, 0.1% Triton X-100, and 50 mM sodium chloride). The discs were counted in a Beckman 4000 γ counter or in a Packard Tri-Carb Model 3375 scintillation spectrometer. When the kinetics of [^{125}I]-α-BuTx binding to receptor (e.g., in the presence of ligand) were measured, the AcChR was incubated for 20–30 min with the desired concentration of the ligand. [^{125}I]-α-BuTx (in excess over receptor) was then added to start the reaction. Aliquots (100 μL) were then taken at given time intervals and pipetted onto DEAE discs which were subsequently transferred into washing buffer and treated as described above. The counts per minute at time t, C_t, are proportional to the amount of receptor–[^{125}I]-α-BuTx complex formed plus a constant additive background, C_b, due to nonspecific binding of toxin (C_b was of the order of 0.5% of the total counts present in the sample). Since the difference $C_\infty - C_t$ (C_∞ = counts per minute measured after completion of the reaction) was considered, the (constant) background canceled.

This method gives a valid measure of the rate of toxin binding only if the reaction is greatly slowed by addition of sample to a DEAE disc. (One might expect that the reaction will be quenched by competition of the high concentration of diethylaminoethyl groups on the disc with toxin for receptor.) That the reaction was indeed quenched upon contact with the DEAE disc was shown as follows. The apparent rate of α-BuTx binding to membrane-bound AcChR was first determined by the DEAE filter disc assay described above. Another receptor–toxin reaction using the same concentrations was then started, and for each time point an aliquot of the reaction mixture was pipetted into a large excess of unlabeled α-BuTx. This resulted in an essentially instantaneous conversion of all free receptor to unlabeled receptor–toxin complex. Because the receptor–toxin reaction is irreversible (see below), the fraction of total receptor–toxin complex due to [^{125}I]-α-BuTx was just the amount of [^{125}I]-α-BuTx–receptor complex formed at the time the reaction was quenched. This concentration was measured by the method of Schmidt & Raftery (1973). Figure 2 shows that the apparent rates of [^{125}I]-α-BuTx binding obtained in the two experiments agreed within 8%, indicating that the DEAE filter assay gives an accurate measure of the toxin binding rate.

Adsorption of the positively charged toxin on the walls of the test tube which has been widely reported in the literature (Colquhoun & Rang, 1976; Bulger et al., 1977) can be minimized by the use of prewashed polystryene test tubes. Routine checks of the total toxin content of the sample showed no significant loss of toxin over a period of several hours at our concentrations (typically 5×10^{-7} M). In the case of membrane-bound AcChR, the experiments were carried out

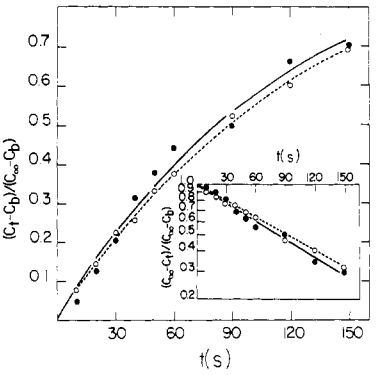

FIGURE 2: Demonstration of quenching of [^{125}I]-α-BuTx binding to AcChR by the DEAE disc assay. The rate of toxin binding was measured by the DEAE disc assay as described under Methods. The data are presented in a normalized form (●) where C_∞ represents the counts per minute bound to a disc at equilibrium and C_b represents a constant, additive background. The reaction mixture was 0.5 μM in [^{125}I]-α-BuTx and 55 nM in α-toxin binding sites. Another reaction, at the same concentration, was started. For each time point, a 50-μL aliquot was pipetted into 75 μL of 50 μM unlabeled α-BuTx with rapid mixing. After all the points had been taken, 100 μL from each point was pipetted onto a DEAE disc and treated as described (see Methods). C_∞ was determined in the same way, while C_b was determined from the intercept ($C_\infty - C_b$) of the semilogarithmic plot of the data. The data (○) are shown as a normalized plot to allow direct comparison with the data determined from the DEAE disc assay (●). The lines were drawn with the rate constants determined by linear least-squares analysis of the semilogarithmic plot of the data. (Insert) Normalized, semilogarithmic plots of the data. The second-order rate constants as determined by linear least-squares analysis of the data were (1.64 ± 0.08) × 10^4 M^{-1} s^{-1} for the disc assay (●) and (1.53 ± 0.04) × 10^4 M^{-1} s^{-1} in the case where the reaction was stopped by an excess of unlabeled toxin (○).

at room temperature in *Torpedo* Ringer's buffer with typical concentrations of [receptor]$_0$ = 5×10^{-8} M in toxin sites and [toxin] = 5×10^{-7} M.

(*5*) *Data Evaluation.* Experimental data were evaluated by the method of (weighted) linear least squares. When nonlinear functions were to be fitted, the weighting factors were recalculated as required for the linearized form of the equation considered, and propagation of errors was calculated according to standard procedures (Bevington, 1969).

When plots of ln ($C_\infty - C_t$) vs. time were found to be nonlinear, the data were fit to an empirical relationship of the form

$$C_\infty - C_t = (C_\infty - C_b)[\alpha \exp(-\lambda_1 t) + (1 - \alpha) \exp(-\lambda_2 t)] \quad (1)$$

where α and $1 - \alpha$ were the fractional amplitudes of two exponentials with decay constants λ_1 and λ_2, respectively, and $C_\infty - C_b$ represented the total amplitude. The quantities C_∞, C_t, C_b, and t are defined in the previous section. Since the two exponentials were well separated, the linear portion of a semilogarithmic plot of the data (see Figure 7B) could be approximated as

$$\ln (C_\infty - C_t) \simeq \ln a - \lambda_2 t \quad (2)$$

where $a = (C_\infty - C_b)(1 - \alpha)$. A linear least-squares analysis according to eq 2 gave estimates for $a \pm \sigma_a$ and $\lambda_2 \pm \sigma_{\lambda_2}$. These values were used to calculate a new function $Y(t)$, linear in time

$$Y(t) = \ln [C_\infty - C_t - a \exp(-\lambda_2 t)] = \ln b - \lambda_1 t \quad (3)$$

where $b = (C_\infty - C_b)\alpha$. Estimates for $b \pm \sigma_b$ and $\lambda_1 \pm \sigma_{\lambda_1}$ were obtained by a weighted linear least-squares analysis of eq 3. Propagation of errors, assuming that the standard deviations in C_∞, C_t, and t were small compared to those of a and λ_2, gave estimates for the variance in $Y(t)$, $\sigma^2_{Y(t)}$, of

$$\sigma^2_{Y(t)} = \frac{\exp(-2\lambda_2 t)[\sigma_a^2 + (at)^2\sigma^2_{\lambda_2}]}{\exp[2Y(t)]} \quad (4)$$

Results and Discussion

(1) Characterization of [^{125}I]-α-BuTx. Chromatography. Following iodination of α-BuTx, the separation obtained by chromatography on a Sephadex CM-25 column at pH 7.4 is shown in Figure 1. Since under the iodination conditions used no modification of histidines in α-BuTx was found by Vogel et al. (1972), only iodination of tyrosine residues was considered. At pH 7.4, diiodotyrosine-containing toxin is separated from toxin containing mono- and unsubstituted tyrosine residues on the basis of differing pK_a values [see e.g., Means & Feeney (1971)]. The radioactive peak centered around fraction 75 in Figure 1 had a variable ratio of protein (measured by absorption at 280 nm) to radioactivity, depending on the preparation, and most likely contained diiodotoxin (Vogel et al., 1972) and inactive toxin fragments. The main peak of radioactivity contained the monoiodotoxin(s) and unlabeled toxin to more than 50% since toxin was in excess over iodine in the reaction mixture (see Methods). This material is referred to as [^{125}I]-α-BuTx.

Localization of [^{125}I]Tyrosine. Isotopic dilutions of two [^{125}I]-α-BuTx preparations were cleaved by cyanogen bromide at Met-27, followed by separation of the resulting fragments (Mebs et al., 1971, 1972). Within the experimental accuracy of the separation, the radioactivity was associated with the second fragment. Since each fragment contains one of the two tyrosine and histidine residues present in α-BuTx (Mebs et al., 1971, 1972), this indicates that in our preparations only Tyr-55 was modified. This is to be expected on the basis of the recent structure determination of a short α-neurotoxin from the Philippine sea snake *Laticauda semifasciata* (Tsernoglou & Petsko, 1976). These authors found that Tyr-25 (located in fragment I) is completely buried in the hydrophobic interior of the protein, whereas Tyr-55 is exposed to the solvent. Moreover, the latter residue is not believed to be of crucial importance for receptor–toxin complex formation (Tsernoglou & Petsko, 1976).

Calibration of [^{125}I]-α-BuTx. Determination of the specific radioactivity of the toxin was achieved by titration with the unlabeled α-BuTx standard (see Methods). Known, subsaturating amounts of the α-BuTx standard were incubated for 30 min with a known amount of purified AcChR. An excess of the radioactive toxin was added, and the solution was incubated for an additional 30 min at room temperature. The receptor-bound radioactivity was determined by the DEAE disc assay (Schmidt & Raftery, 1973) (see Figure 3).

The radioactivity bound (C^*, in cpm/mL) is then related to the number of receptor binding sites by $C^* = AR$ where A is the experimentally determined specific activity of the toxin and R is the number of toxin binding sites.

If R_0 represents the total number of binding sites in the initial receptor solution, and if T is the amount of unlabeled toxin added, then $R = R_0 - T$ and

$$C^* = A(R_0 - T) \quad (5)$$

Therefore, a plot of C^* vs. T (see insert of Figure 3) will be linear with a slope of $-A$ and an intercept at the abscissa equal to R_0, the number of α-BuTx binding sites present in the purified AcChR solution. In this case, the specific activity was 8×10^{12} cpm/mmol at a counting efficiency of 78%.

The concentration of the [^{125}I]-α-BuTx stock solution was determined by measuring the amount of radioactive complex C^* formed when solubilized AcChR was in excess over a known amount of the radioactive toxin. Since $C^* = AT_0$, the amount of [^{125}I]-α-BuTx added, T_0, can be calculated. This value for T_0 was compared with those determined by the method of Lowry et al. (1951) and by Fluram assay. The results of the three determinations showed good agreement. The yield of the iodination reaction was typically 50% of the theoretical. The stock solution of [^{125}I]-α-BuTx was stored refrigerated and was stable over a period of at least 5 months. Three calibrations of this preparation showed no significant deviation from the theoretical decay curve of ^{125}I over this period. Also, gel filtration on a Sephadex G-25 column of the 5-month-old [^{125}I]-α-BuTx showed a single sharp peak in the void volume as assayed by radioactivity and Fluram.

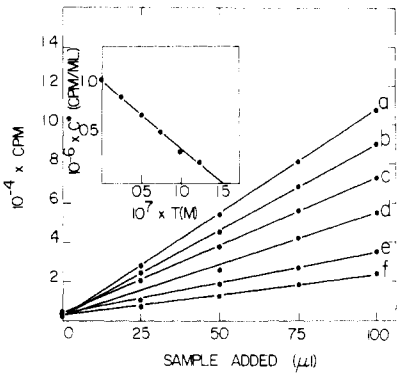

FIGURE 3: Determination of the specific activity of [^{125}I]-α-BuTx. Six solutions (a–f) of solubilized, purified receptor (~0.16 μM in α-toxin sites) containing from 0 to 0.125 μM unlabeled α-BuTx were prepared in washing buffer. After 0.5 h, aliquots of these solutions were mixed with 25 μL of a 50-fold dilution of the [^{125}I]-α-BuTx to be calibrated, and the volumes were adjusted to 125 μL with washing buffer. Following an additional 30-min incubation, the receptor-bound radioactivity was determined by the DEAE disc assay. For each of the solutions a–f, a plot of radioactivity bound vs. volume of sample added gave a straight line whose slope [C^* (cpm/mL)] was a measure of the concentration of free receptor sites remaining after reaction with the unlabeled toxin. (Insert) C^* was plotted vs. the concentration of unlabeled toxin added (T). The specific activity of the toxin was than 1.25 times the slope of this line. This factor of 1.25 was due to the fact that only 100 μL of each sample (125 μL total) was pipetted onto the disc.

(2) Kinetic Homogeneity of [^{125}I]-α-BuTx. As discussed in section 1, the radioactive toxin preparation contained unlabeled toxin (to more than 50%), monoiodinated toxin (labeled at Tyr-55), and conceivably other monoiodinated toxin species. The possibility that such chemical heterogeneity of [^{125}I]-α-BuTx could lead to kinetic heterogeneity in its reaction with membrane-bound AcChR was tested in the following experiment. Various isotopic dilutions of [^{125}I]-α-BuTx (at a constant total toxin concentration) were incubated with different amounts of receptor as described in the legend to Figure 4, and the total amount of radioactive complex at equilibrium was assayed by the procedure of Schmidt & Raftery (1973).

We first consider the case when [^{125}I]-α-BuTx contains only two species of toxin (i.e., unlabeled T and monolabeled T*). If each species binds irreversibly to the same class of receptor sites in the membranes (see next section), then the parallel reactions

$$R + T \xrightarrow{k_1} C; \qquad R + T^* \xrightarrow{k_2} C^* \quad (6)$$

will occur where R denotes the AcChR sites, C and C* are the receptor–toxin complexes, and k_i are the respective second-order rate constants. Dividing the rate equations pertaining to eq 6, one obtains the relation

$$\frac{dC^*}{T^*_0 - C^*} = q_2\frac{dC}{T_0 - C}$$

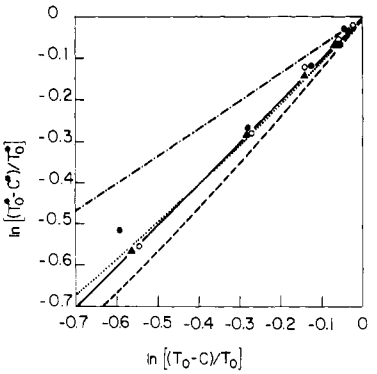

FIGURE 4: Kinetic homogeneity of [^{125}I]-α-BuTx binding to membrane-bound AcChR. AcChR at five different concentrations (R_0 = 8.4 × 10^{-7}, 4.2 × 10^{-7}, 2.1 × 10^{-7}, 1.05 × 10^{-7}, and 5.025 × 10^{-8} M) was incubated with three different isotopic dilutions of [^{125}I]-α-BuTx at a constant total toxin concentration of 1.8 × 10^{-6} M. (▲) Undiluted [^{125}I]-α-BuTx. (○) [[^{125}I]-α-BuTx]$_0$ = [α-BuTx]$_0$ = 9 × 10^{-7} M and (●) [[^{125}I]-α-BuTx]$_0$ = 4.5 × 10^{-7} M and [α-BuTx]$_0$ = 1.35 × 10^{-6} M. The concentration of radioactive complex at equilibrium, C^*, was determined by the method of Schmidt & Raftery (1973). Data are presented as a plot of ln $[(T^*_0 - C^*)/T^*_0]$ vs. ln $[(T_0 - C)/T_0]$, where T^*_0 and T_0 were accurately known and C was calculated from $C = R_0 - C^*$. The data are fit by a straight line with slope unity (—). For comparison, plots of eq 7A are shown with the parameters $q_2 = 1$ and $q_3 = 1.5$ (---); $q_1 = 1$ and $q_3 = {}^2/_3$ (····); and $q_2 = 0.87$ and $q_3 = 1.37$ (···) with $T^*_{2(0)}/T^*_0 = T^*_{3(0)}/T^*_0 = 0.5$ in all cases (see text).

where the subscript 0 refers to the initial concentration of the toxins and $q_2 = k_2/k_1$. Integration with the initial conditions $C(0) = C^*(0) = 0$ leads to the equation (at equilibrium)

$$\ln [(T^*_0 - C^*)/T^*_0] = q_2 \ln [(T_0 - C)/T_0] \quad (7)$$

Therefore, a plot of ln $[(T^*_0 - C^*)/T^*_0]$ vs. ln $[(T_0 - C)/T_0]$ should be linear with slope q_2 and an intercept of 0.

The experimental data are shown in Figure 4. They are fit by a straight line with slope unity. Therefore, the labeled toxin binds with the same rate constant to the receptor as does the unlabeled toxin. When total toxin concentration is in excess over receptor, C and C^* are given by

$$C^* = R_0 T^*_0/(T_0 + T^*_0); \qquad C = R_0 T_0/(T_0 + T^*_0) \quad (8)$$

Reinsertion of the formulas into eq 8 gives

$$\ln [(T^*_0 - C^*)/T^*_0] = \ln [(T_0 - C)/T_0] = \ln [1 - R_0/(T_0 + T^*_0)] \quad (9)$$

The data points in Figure 4 should then depend only on the ratio of the total amounts of toxin sites to toxin molecules, independent of the isotopic dilution chosen. Figure 4 shows that this prediction is indeed fulfilled.

We may extend the above analysis by considering that, in addition to the unlabeled species T, there are two monolabeled toxins T^*_2 and T^*_3 reacting with rate constants k_2 and k_3, respectively. In this case one obtains two equations analogous to eq 7 for the radioactive receptor–toxin complexes C^*_2 and C^*_3. For the experimentally observable quantity $C^* = C^*_2 + C^*_3$, the total concentration of radioactive complex at equilibrium (note that T_2 and T_3 have the same specific activity, both being monoiodinated species), one obtains

$$\ln \frac{T^*_0 - C^*}{T^*_0} = q_2 \ln \frac{T_0 - C}{T_0} + \ln \left[\frac{T^*_{2(0)}}{T^*_0} + \frac{T^*_{3(0)}}{T^*_0} \left(\frac{T_0 - C}{T_0} \right)^{(q_3 - q_2)} \right] \quad (7A)$$

where $T^*_0 = T^*_{2(0)} + T^*_{3(0)}$, and $q_i = k_i/k_1$. In general then, a plot such as that shown in Figure 4 will be nonlinear. However, if $q_2 = q_3$, eq 7A reduces to eq 7 and the plot will be linear. Since $(T_0 - C)/T_0 < 1$ the plot will also approach linearity if $q_3 \gg q_2$. Under these conditions the plot in Figure 4 will also have slope q_2, but the intercept will be ln $(T^*_{2(0)}/T^*_0) < 0$. Therefore, this case may be excluded as long as there is a sizable fraction of T^*_3 ($T^*_3/T^*_0 > 10\%$).

Figure 4 also demonstrates the behavior of eq 7A under conditions where $q_2 \neq q_3$. Two plots are shown with the parameters $T^*_{3(0)}/T^*_0 = {}^1/_2$, $q_2 = 1$, and q_3 = either 1.5 (---) or ${}^2/_3$ (····) so that T^*_3 reacts 50% faster or slower than T and T^*_2. These curves show little deviation from linearity but differ in slope from the case $q_2 = q_3 = 1$ (—). It is indeed possible to fit the experimental data by adjusting q_2 and keeping $q_3 - q_2$ constant [Figure 4 (···)]. However, plots of eq 7A for $q_3 - q_2 = 1$ or $-{}^1/_2$ (not shown) exhibit a pronounced nonlinearity and can no longer be brought into agreement with the data by any choice of q_2. It is concluded that a kinetic heterogeneity of two radioactive toxin species will be detected as long as they are present in approximately equal amounts and their rate constants for toxin binding differ by a factor of two or more. The extension of this analysis to more complex toxin mixtures is possible, but it will have a lower power of resolution.

The essential assumptions for the method presented above are that (a) there is only one class of binding sites and (b) complex formation *can be regarded* as irreversible. When dissociation of the complexes cannot be neglected, the above analysis, which considers the radioactivity bound at equilibrium, must obviously be replaced by an appropriate kinetic method. That receptor toxin complex formation is irreversible is also essential for the applicability of the calibration procedure described in the previous section. In the case of a reversible reaction, the determination of the specific activity of T* is also possible by the method of isotopic dilution outlined above. Assuming that the equilibrium constant for both T and T* is the same, we would replace eq 5 by $C^*/C = A(T^*/T)$. If the total toxin concentration is always in large excess over receptor, $(T_0 + T^*_0) \gg R_0$, this equation can be easily evaluated.

(3) [^{125}I]-α-BuTx Binding to Membrane Bound AcChR. Figure 5A shows semilog plots of the kinetics of [^{125}I]-α-BuTx binding to the membrane-bound receptor for varying toxin concentrations in large excess. The plots are linear within the time the reaction was followed (up to 90%), indicating a kinetically homogeneous class of toxin binding sites as assumed in the previous section. Linear least-squares analysis of these data gives the apparent rate of toxin binding, k_{app}. Figure 5B shows the concentration dependence of k_{app} in the form of a double logarithmic plot. Weighted linear least-squares analysis of these data gives a slope of 0.98 ± 0.02. This means that, up to the experimentally reached concentrations of 3 μM, k_{app} varies linearly with toxin concentration

$$k_{app} = kT_0 \quad (10)$$

The second-order rate constant, k, is determined from a linear plot of k_{app} vs. T_0 to be (1.2 ± 0.1) × 10^4 M^{-1} s^{-1}.

Figure 5B shows that toxin binding kinetics to membrane fragments shows no deviation from the simple mechanism

$$R + T \xrightarrow{k} RT \quad (11)$$

in the experimentally accessible concentration range.

A simple bimolecular mechanism for toxin binding to membrane-bound receptor was also found by Weber & Changeux (1974), Colquhoun & Rang (1976), and Weiland et al. (1976) using a more limited concentration range. This

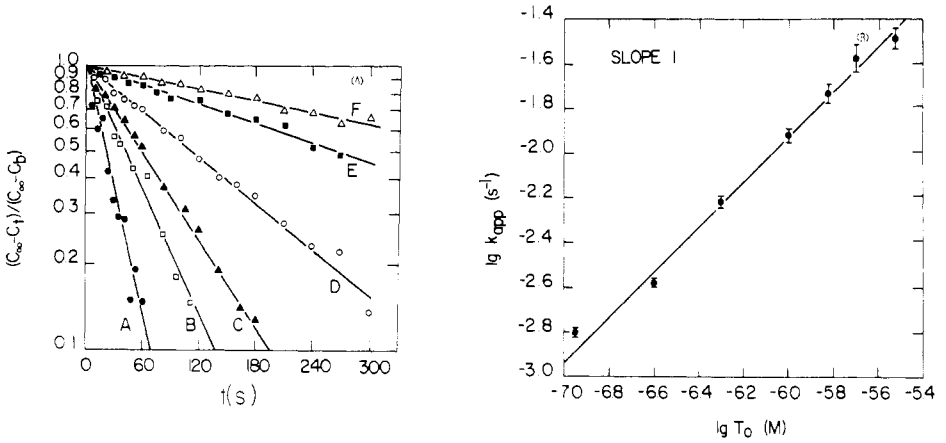

FIGURE 5: (A) Kinetics of [^{125}I]-α-BuTx binding to membrane-bound AcChR with toxin in varying excess over receptor. Data are presented in the form of normalized semilogarithmic plots, corrected for background [C_t and C_∞ = counts per minute at time t and at equilibrium, respectively, containing the same constant background C_b (see Methods)]. The concentrations were as follows: $R_0 = 5 \times 10^{-8}$ M in toxin sites (A–D) or 2.5×10^{-8} M (E and F); $T_0 = 3 \times 10^{-6}$ M (A), 1.5×10^{-6} M (B), 1.0×10^{-6} M (C), 5×10^{-7} M (D), 2.5×10^{-7} M (E), and 1.25×10^{-7} M (F). The slopes were determined from a linear least-squares fit and gave the apparent rate constants of toxin binding, k_{app}. (B) Dependence of the apparent rate constant of toxin binding, k_{app}, as a function of toxin in excess. Weighted linear least-squares analysis of a double logarithmic plot of the data gave a slope of 0.98 ± 0.02. This indicated that k_{app} was proportional to T_0.

result is, however, contrary to that found by Bulger et al. (1977) for the interaction of [^{125}I]-α-BuTx with membrane-bound AcChR from *Electrophorus*. Those authors found biphasic toxin kinetics and explained their data by an allosteric model of the AcChR with toxin acting as an allosteric modifier. Except for species-related differences between *Torpedo* and *Electrophorus*, no simple explanation can be given for the conflicting observations.

The observed value of the second-order rate constant of toxin binding is rather low for a simple bimolecular association. This phenomenon can be explained in part by the strong inhibition of toxin binding due to Ca^{2+}, Mg^{2+}, and monovalent cations. Decreasing the concentrations of Ca^{2+}, Mg^{2+}, and Na^+ leads to an acceleration of the toxin kinetics by more than an order of magnitude (Deutsch, 1976). Similar phenomena have been observed with solubilized AcChR (Schmidt & Raftery, 1974). We cannot exclude the possibility, however, that a more complex mechanism (e.g., fast preequilibria with equilibrium constants $> 10^{-5}$ M) gives rise to the low rate constant.

The complex formed from membrane-bound AChR and [^{125}I]-α-BuTx is very stable. Addition of a 500-fold (molar) excess of unlabeled toxin to a freshly prepared [^{125}I]-α-BuTx–receptor complex solution did not result in any significant loss of receptor-bound radioactivity over a period of 2 days. The long lifetime of the receptor–toxin complex seems to be characteristic of the membrane-bound AcChR.

(4) Effects of Cholinergic Ligands on [^{125}I]-α-BuTx Binding to Membrane-Bound Receptor. The inhibition of the toxin binding rate by varying concentrations of cholinergic ligands is shown in Figure 6. When we assume that ligand binding is (a) competitive and (b) in fast preequilibrium with toxin binding, the kinetics under pseudomonomolecular conditions ($T_0 \gg R_0$) will be monophasic. The observed rate of toxin binding in the presence of ligand, $k_{app}(L)$, is

$$k_{app}(L) = k[T_0(1 + L/K_i)^{-1}] \qquad (12)$$

where L is the concentration of free ligand and K_i denotes the apparent equilibrium constant for the ligand. The other symbols are defined in eq 8. Figure 6 shows that the data are reasonably fit by eq 10. The parameters K_i, obtained from a weighted linear least-squares fit to the linearized form of eq 12 (see caption of Figure 6), are listed in Table I. In general, they are in good agreement with the values found by others using toxin inhibition (see e.g., Weber & Changeux,

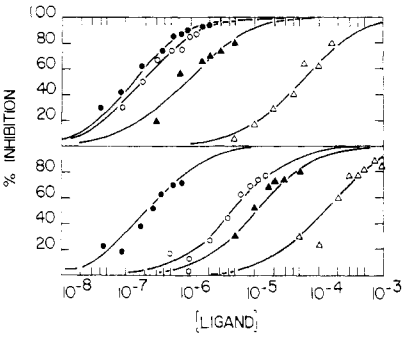

FIGURE 6: Inhibition of toxin binding kinetics to membrane-bound AcChR as a function of free ligand concentration. Membrane fragments (50–60 nM in toxin sites normally in the low affinity form) were incubated with ligand for 20–30 min. The reaction was started by adding a 10-fold excess of [^{125}I]-α-BuTx, and the kinetics of toxin binding were followed to at least 50% completion. Semilogarithmic plots of these data showed no systematic deviation from a straight line, and the slopes were evaluated by a linear least-squares fit, yielding the apparent rate constant of toxin binding in the presence of ligand, $k_{app}(L)$. The plot shows the inhibition of the toxin kinetics defined as $1 - k_{app}(L)/k_{app}$ ($L = 0$) (in %) as a function of free ligand concentration. (Upper panel) Agonists: Carb (●), Deca (○), nicotine (▲), and choline (△). (Lower panel) Antagonsts: *d*-Tc (●), DAP (○), flaxedil (▲), and Hexa (▲). The curves were calculated by a weighted linear least-squares fit to the linearized form form of eq 3 $[k_{app}(L)]^{-1} = [k_{app}(L = 0)]^{-1}(1 + L/K_i)$. The calculated inhibition constants, K_i, are listed in Table I.

Table I: Inhibition of Toxin Binding to Membrane-Bound AcChR by Cholinergic Ligands

ligand	pharmacological act.	K_i[a] (M)
Carb	agonist	$(1.2 \pm 0.2) \times 10^{-7}$
Deca	agonist	$(1.8 \pm 0.1) \times 10^{-7}$
nicotine	agonist	$(9.3 \pm 1.1) \times 10^{-7}$
choline	agonist	$(5.1 \pm 0.4) \times 10^{-5}$
d-TC	antagonist	$(2.0 \pm 0.4) \times 10^{-7}$
DAP	antagonist	$(4.7 \pm 0.3) \times 10^{-6}$
flaxedil	antagonist	$(1.1 \pm 0.1) \times 10^{-5}$
Hexa	antagonist	$(1.2 \pm 0.14) \times 10^{-4}$

[a] K_i determined from the inhibition of the initial rate of toxin binding according to eq 12 (see caption of Figure 6 for details).

1974; Quast et al., 1978b). When the fraction of ligand bound could not be neglected ($K_i \simeq R_0 \simeq 5 \times 10^{-8}$ M), the concentration of free ligand L was calculated by the law of mass

Table II: Kinetics with Solubilized, Purified Receptor[a]

concn (nM)[b]					
R_0	T_0	δA_1 (%)	$k_1 \times 10^{-5}$ (M^{-1} s^{-1})	δA_2 (%)	$k_2 \times 10^{-4}$ (M^{-1} s^{-1})
52	5.8	100	2.9 ± 0.25		
5.5	56	35 ± 18	3.7 ± 2[c]	65 ± 20	7.8 ± 1.5
8.1	94	39 ± 11	3.0 ± 1.1	61 ± 12	6.6 ± 1.1

[a] Experiments were carried out in *Torpedo* Ringer's solution, containing 0.1% Triton X-100. The δA_i (in % of δA_t) and k_i were determined by the linear least-squares procedure outlined under Experimental Section. [b] R_0 = concentration in toxin *sites*. [c] Mean value determined for two different AcChR preparations.

action. When a stoichiometry of toxin to ligand sites of 2:1 was assumed (see below), these corrections changed the final value of K_i by less than 15% (or 20% in the case of a 1:1 stoichiometry).

Of the two assumptions necessary for eq 12, competition between ligands and toxin for the AcChR is more important. Even if the condition of fast preequilibrium is not met, the initial slope of toxin binding will follow eq 12, since the concentration of free receptor is reduced to $R_0(1 + L/K_i)^{-1}$ in the presence of ligand. Competition with toxin, *in principle*, can be shown for every ligand by verification of the kinetic formula (eq 12) under varying toxin and ligand concentrations as well as by equilibrium measurements of the amount of toxin bound in the presence of sufficiently high ligand concentrations.

In the case of Carb, a detailed study has shown eq 12 to apply (Quast et al., 1978b), although the ratio of toxin to ligand sites is 2:1 (Raftery et al., 1975; Quast et al., 1978a). Ultracentrifugation experiments with [^{3}H]Carb show that binding of toxin and Carb to membrane-bound AcChR are mutually exclusive at equilibrium (Schimerlik et al., unpublished observations). The molecular mechanism of this inhibition is, however, not understood because of the stoichiometry of toxin to Carb sites. A stoichiometry of 2:1 has also been found for Deca and *d*-Tc when the fluorescent probe Eth is used (Schimerlik et al., 1979). Further evidence for mutual exclusion of toxin and other cholinergic ligands (Deca or *d*-Tc) has been given by Weber & Changeux (1974). A ratio of 2:1 for the number of toxin to cholinergic ligand sites has also been found in the case of solubilized AcChR (Moody et al., 1973; Maelicke et al., 1977).

Whatever the inhibition mechanism involved, the dissociation constants calculated from eq 10 are in good agreement with the equilibrium constants found with radiolabeled ligands (e.g., Carb; Raftery et al., 1975) as well as values from the ligand-induced fluorescence increase of receptor-bound Eth (Quast et al., 1978a; Schimerlik et al., 1979). Elucidation of the details of both ligand binding mechanisms and of toxin inhibition will require development of a more precise assay which allows continuous study of this complex three-component system.

(5) *Kinetics of Toxin Binding to Solubilized, Purified AcChR.* Semilogarithmic plots of the toxin binding kinetics to solubilized, purified receptor where (a) receptor was in large excess over toxin and (b) toxin was in excess over receptor are shown in Figure 7A and 7B, respectively. Clearly, there was a significant deviation from linearity when toxin was in excess over receptor, thus ruling out the simple bimolecular mechanism (eq 11) which described toxin binding to the membrane-bound AcChR. The limited resolution of the DEAE disc assay in the fast time domain (s) and the inevitable scatter in C_t observed near completion of the reaction made accurate

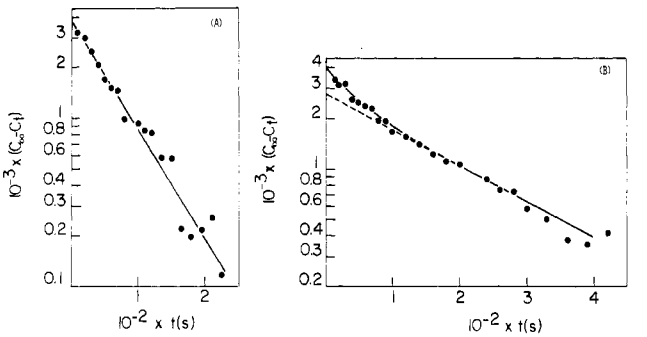

FIGURE 7: (A) Kinetics of [^{125}I]-α-BuTx binding to solubilized, purified AcChR with receptor in excess over toxin. Data are presented as a semilogarithmic plot. The solid line was determined by linear least squares as described under Methods. The concentrations of receptor and [^{125}I]-α-BuTx were 52 and 5.8 nM, respectively. (B) Kinetics of [^{125}I]-α-BuTx binding to solubilized, purified AcChR with toxin in excess over receptor. A semilogarithmic plot of the data shows clear biphasicity. The solid line was fit as described under Methods and extrapolates to log ($C_\infty - C_b$) at time zero. An extrapolation of the slow phase to time zero (dotted line) yields the value for $\delta A_2(C_\infty - C_b)$. The concentrations were R_0 = 5.2 nM and T_0 = 56 nM.

experiments under conditions of high toxin very difficult and severely restricted the accessible concentration range. The kinetic parameters obtained from experiments as shown in Figure 7 are listed in Table II.

Any mechanism proposed to fit these data must predict biphasic kinetics with approximately equal amplitudes δA_1 and δA_2 for the two phases when toxin is in excess over receptor, and, in the case of low receptor occupancy, $R_0 \gg T_0$, the predicted kinetics must degenerate to a single exponential. This type of kinetic behavior is a feature of the following two models.

Model A

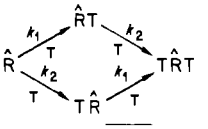

(13)

assumes two classes of independent sites for toxin on the receptor: Here R̂ is an entity which binds two molecules of toxin, R̂T and TR̂ are the different monotoxin complexes, TR̂T is the ditoxin complex, and k_1 and k_2 are the association rate constants for toxin combining with the two different sites.

Model B assumes negative cooperativity for the binding of toxin. Binding of a first molecule of toxin to the (orginally identical) binding sites of R̂ renders binding of the second molecule more difficult. (The molecular basis for the negative cooperativity could be steric hindrance or a conformational change after the first toxin molecule has bound.) The model reads

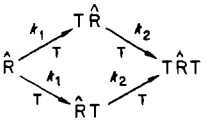

(14)

where k_1, the microscopic association rate constant for formation of the (identical) monotoxin complexes R̂T = TR̂, now contains a statistical weight of 2 as compared to the k_1 in eq 13, where the two toxin sites were intrinsically different. Therefore, the numerical value for k_1 in eq 14 is $^1/_2$ that of k_1 in eq 13. The kinetic schemes 13 and 14 can be solved by standard methods for the experimentally observed quantity

$$z = \hat{R}T + T\hat{R} + 2\,T\hat{R}T \qquad (15)$$

in the cases $\hat{R}_0 \gg T_0$ and $\hat{R}_0 \ll T_0$. The results are listed in

Table III: Time Dependence of the Observable $z = \hat{R}T + T\hat{R} + 2T\hat{R}T$ According to the Two-Sites Model (eq 13) and the Negative Cooperative Model (eq 14)

model	expt condition	$z(t)$
two classes of sites, model 13	$T_0 << \hat{R}_0$	$z = T_0\{1 - \exp[-(k_1 + k_2)[\hat{R}_0 t]\}$
	$T_0 >> \hat{R}_0$	$z = 2\hat{R}_0\{1 - {}^1/_2 \exp(-k_1 T_0 t) - {}^1/_2 \exp(-k_2 T_0 t)\}$
negative cooperative, model 14	$T_0 << \hat{R}_0$	$z = T_0\{1 - \exp(-2k_1 \hat{R}_0 t)\}$
	$T_0 >> \hat{R}_0$	$z = 2R_0\{1 - {}^1/_2 \cdot \frac{r-2}{r-1}[\exp(-2k_1 T_0 t)] - {}^1/_2 \frac{r}{r-1}[\exp(-k_2 T_0 t)]\}$

Table III. One sees that at low receptor occupancy both mechanisms predict a single exponential (note the statistical factor of 2 in the apparent rate constant in the case of the negatively cooperative model). With toxin in excess over receptor, it is apparent that, within the error limits, the two-site model (13) is in fair agreement with the experimental observations given in Table II since it predicts $\delta A_1 = \delta A_2$ ($= {}^1/_2$) and that the apparent rate constants, $k_{app}(i)$, vary linearly with the toxin concentration in excess so that $k_{app}(i)/T_0 = k_i$ = constant (see Table II). The (mean) values are $k_1 = (3.4 \pm 1.6) \times 10^5$ M^{-1} s^{-1} for the fast and $k_2 = (7.2 \pm 1.3) \times 10^4$ M^{-1} s^{-1} for the slow phase. Furthermore, the experimental value of the second-order rate constant observed with receptor in excess agrees, within the statistical error, with the rate constant k_1 for the fast phase of the biphasic kinetics appearing with toxin in excess. This is to be expected (see Table II) since k_1 is about five times larger than k_2. The negatively cooperative model also correctly predicts the observed difference between high toxin and high receptor kinetics (see Table III). The calculated concentration dependence of the relaxation rates is theoretically indistinguishable from that obtained by assuming independent sites. The amplitudes of the fast phase, δA_1, for this model with $R_0 \ll T_0$ is given by $\delta A_1 = {}^1/_2(r - 2)/(r - 1)$ (see Table III). With $r = 4.7 \pm 2.4$ one calculates $\delta A_1 = 0.365 \pm 0.088$. This value is in good agreement with the experimental mean of $\delta A_1 = 0.37 \pm 0.15$ (from Table II), and therefore this model seems to be favored. The low precision of these data, however, does not allow one to discriminate between the two models (schemes 13 and 14) at this point.

In addition, the limited concentration range accessible under the present conditions does not allow us to exclude more complex models where, with toxin in excess, the ratio of $\delta A_1/\delta A_2$ would depend on toxin concentration or where fast preequilibria would precede slow isomerization steps. An assay capable of improved time resolution would be necessary to allow a choice between schemes 13 and 14, or one of the more complex possibilities.

Because of the inherent complexities of the toxin binding kinetics with solubilized, purified receptor and the difficulties encountered in the experiments, we have not attempted a quantitative description of the inhibition by cholinergic ligands. Qualitative observations with toxin in excess indicate that ligands inhibit the fast phase less than the slow with DAP being the extreme case [see, e.g., Raftery et al. (1975)]. In general, the concentrations of agonists required to decrease the rate of toxin binding to solubilized, purified receptor are much higher than those necessary with membrane-bound AcChR, while antagonists exhibit a lesser difference (Raftery et al., 1975; Vandlen et al., 1976).

(6) *Conclusion.* The main objective of this study has been to show that valuable quantitative information on the kinetics of toxin binding to the receptor and its inhibition by cholinergic ligands could be obtained once the radiolabeled toxin derivative was carefully characterized and a quantitative assay for toxin binding was developed. One intriguing result of this work was the striking difference between membrane-bound and solubilized AcChR. Whereas toxin binding kinetics to the membrane-bound receptor did not deviate from the simple bimolecular association mechanism (eq 11) to a single class of noninteracting sites under the experimental conditions used, the reaction of toxin with solubilized AcChR showed heterogeneous kinetics when toxin was in excess over receptor. Two different models, assuming either two independent classes of sites or interdependent sites with negative cooperativity, were in agreement with the observed phenomena. Whatever the molecular basis for this kinetic heterogeneity might be, it seems to be induced by the solubilization and purification process of the AcChR. This assumption is supported by the observation that addition of 0.5% chloroform and 0.5% ethanol to membrane-bound AcChR induces a strong biphasicity of the toxin kinetics, affecting (about) half of the sites (H. P. Moore, unpublished experiments). At high cholate concentrations in membrane fragment extracts, about half of the sites are not available for toxin binding but can be recovered upon dilution (R. Vandlen and J. Miller, unpublished experiments). Taken together, these findings strongly support the idea that perturbation of the receptor's lipid environment is the cause of the observed kinetic heterogeneity. In principle, two modes of action seem plausible for these perturbants. (a) Addition of the agent directly modifies half of the toxin sites which are more sensitive to protein–lipid interactions; thus, heterogeneity of toxin sites ab initio would be induced by these perturbants and eq 13 would apply. (b) The perturbants cause a general conformational change in the receptor protein, inducing a conformation in which binding of a first toxin molecule to one of the (originally equivalent) sites *sterically* inhibits binding of a second toxin molecule (eq 14). The possibility that the negative cooperativity model (eq 14) reflects a regulatory property of the solubilized (or perturbed) AcChR (i.e., inhibition of a second toxin molecule binding due to conformational change occurring in the monotoxin complex) is unappealing, since it is difficult to imagine that solubilization and affinity chromatography might have added a regulatory property to the receptor that the molecule did not possess in its native membrane environment.

Further differences between the toxin kinetics observed with solubilized, purified or the membrane-bound AcChR lie in the values of the second-order rate constants found for the two preparations. Solubilized receptor binds toxin about 15 times faster than membrane-bound receptor for the fast phase and four times faster than the slow phase. Since the buffers used differed only by the presence of 0.1% (v/v) Triton X-100 for the case of solubilized, purified receptor, salt effects on the toxin binding rate previously observed for solubilized, purified receptor could be ruled out (Schmidt & Raftery, (1974). Apart from any (unknown) effects of Triton, the observed differences in rate constants might be due to (a) different conformations for the solubilized, purified and the membrane-bound receptor, with toxin binding to the solubilized conformation being faster or (b) the fact that the solubilized receptor is homogeneously distributed in the reaction volume, whereas the membrane-bound receptor is not.

The information on ligand binding to the AcChR obtained by the toxin inhibition method is indirect, and a quantitative

interpretation of the data depends on the molecular nature of the inhibition mechanism. Since the mechanism of toxin binding itself is different for membrane-bound and purified receptor, it is not surprising that there are even greater differences in ligand binding to the two receptor preparations as reflected by toxin binding inhibition. A most significant difference is that the (slow) time-dependent increase of ligand affinity toward the membrane-bound receptor has not been observed for Triton-solubilized, purified receptor. Comparison of the equilibrium constants for ligand binding to the membrane-bound (Table I) and solubilized receptor (Raftery et al., 1975; Vandlen et al., 1976) shows that the values found for antagonists agree within 1 order of magnitude for both receptor preparations, whereas very large differences are found in the respective values for agonists.

Since the solubilized receptor is unable to undergo the ligand-induced conformational change observed in membrane-bound AcChR (Weber et al., 1975; Weiland et al., 1976; Lee et al., 1977; Quast et al., 1978b) and this transition is most prominent with agonists (Weber et al., 1975; Quast et al., 1978b), it seems plausible that large differences in (overall) equilibrium constants are observed for agonists between the two receptor preparations, whereas the values for antagonists are in much closer agreement.

Acknowledgments

The authors are grateful to Dr. Veit Witzemann for determination of the lifetime of the iodinated receptor–toxin complex and to Janet Elliott for her assistance in the calibration of the radioactive toxins. We also thank Wilson Wu and James Eisenach for the amino acid analyses and John Racs for his technical assistance.

References

Bevington, P. R. (1969) *Data Reduction and Error Analysis for the Physical Sciences*, especially Section 9.3, McGraw-Hill, New York.

Bulger, J. E., Fu, J. J. L., Hindy, E. F., Silberstein, R. L., & Hess, G. P. (1977) *Biochemistry 16*, 684–692.

Chicheportiche, R., Vincent, J.-P., Kopeyan, C., Schweitz, H., & Lazdunski, M. (1975) *Biochemistry 14*, 2081–2091.

Clark, D. G., Macmurchie, D. D., Elliott, E., Wolcott, R. G., Landel, A. M., & Raftery, M. A. (1972) *Biochemistry 11*, 1663–1668.

Colquhoun, D., & Rang, H. P. (1976) *Mol. Pharmacol. 12*, 519–535.

Deutsch, J. (1976) Thesis, California Institute of Technology, Pasadena, CA.

Duguid, J. R., & Raftery, M. A. (1973) *Biochemistry 12*, 3593–3596.

Laemmli, U. K. (1970) *Nature (London) 270*, 680–685.

Lee, C. Y., & Chang, C. C. (1966) *Mem. Inst. Butantan Symp. Int. 33*, 555.

Lee, C. Y., Tseng, F. F., & Chiu, T. H. (1967) *Nature (London) 215*, 1177–1178.

Lee, T., Witzemann, V., Schimerlik, M. I., & Raftery, M. A. (1977) *Arch. Biochem. Biophys. 183*, 57–63.

Lowry, O. H., Rosenbrough, N. J., Farr, A., & Randall, R. J. (1951) *J. Biol. Chem. 193*, 265–275.

Maelicke, A., Fulpius, B. W., Klett, R. P., & Reich, E. (1977) *J. Biol. Chem. 252*, 4811–4830.

Means, G. E., & Feeney, R. E. (1971) *Chemical Modification of Proteins*, p 179, Holden-Day, San Francisco.

Mebs, D., Narita, K., Iwanaga, S., Samejima, Y., & Lee, C. Y. (1971) *Biochem. Biophys. Res. Commun. 44*, 711–716.

Mebs, D., Narita, K., Iwanaga, S., Samejima, Y., & Lee, C. Y. (1972) *Hoppe-Seyler's Z. Physiol. Chem. 353*, 243–262.

Meunier, J. C., Sealock, R., Olsen, R., & Changeux, J.-P. (1974) *Eur. J. Biochem. 45*, 371–394.

Moody, T., Schmidt, J., & Raftery, M. A. (1973) *Biochem. Biophys. Res. Commun. 53*, 761–772.

Mooser, G., Schulman, H., & Sigman, D. S. (1972) *Biochemistry 11*, 1595–1602.

Quast, U., Schimerlik, M. I., & Raftery, M. A. (1978a) *Biochem. Biophys. Res. Commun. 81*, 955–963.

Quast, U., Schimerlik, M. I., Lee, T., Witzemann, V., Blanchard, S. G., & Raftery, M. A. (1978b) *Biochemistry 17*, 2405–2414.

Raferty, M. A., & Cole, R. D. (1963) *Biochem. Biophys. Res. Commun. 10*, 467–472.

Raftery, M. A., Vandlen, R. L., Reed, K. L., & Lee, T. (1975) *Cold Spring Harbor Symp. Quant. Biol. 40*, 193–202.

Reed, K., Vandlen, R. L., Bode, J., Duguid, J. R., & Raftery, M. A. (1975) *Arch. Biochem. Biophys. 167*, 138–144.

Schimerlik, M., Quast, U., & Raftery, M. A. (1979) *Biochemistry* (sixth of 10 papers in this series).

Schmidt, J., & Raftery, M. A. (1973) *Anal. Biochem. 52*, 349–354.

Schmidt, J., & Raftery, M. A. (1974) *J. Neurochem. 23*, 617–623.

Steers, E., Craven, G. R., & Anfinsen, C. (1965) *J. Biol. Chem. 240*, 2478–2884.

Tsernoglou, D., & Petsko, G. A. (1976) *FEBS Lett. 68*, 1–4.

Vandlen, R. L., Schmidt, J., & Raftery, M. A. (1976) *J. Macromol. Sci., Chem. 10*, 73–109.

Vogel, Z., Sytkowski, A. J., & Nirenberg, M. W. (1972) *Proc. Natl. Acad. Sci. U.S.A. 69*, 3180–3184.

Weber, M., & Changeux, J.-P. (1974) *Mol. Pharmacol. 10*, 15–34.

Weber, M., David Pfeuty, T., & Changeux, J.-P. (1975) *Proc. Natl. Acad. Sci. U.S.A. 72*, 3443–3447.

Weiland, G., Georgia, B., Wee, V. T., Chignell, C. F., & Taylor, P. (1976) *Mol. Pharmacol. 12*, 1091–1105.

Weiland, G., Georgia, B., Wee, V. T., Chignell, C. F., & Taylor, P. (1977) *J. Biol. Chem. 252*, 7648–7656.